Stem Cell Reviews and Reports
https://doi.org/10.1007/s12015-022-10356-6

Induction of Corneal Epithelial Differentiation of Induced Pluripotent and Orbital Fat-Derived Stem Cells Seeded on Decellularized Human Corneas

Thaís Maria da Mata Martins[1] · Juliana Lott de Carvalho[2,3] · Pricila da Silva Cunha[4,5] · Dawidson Assis Gomes[4] · Alfredo Miranda de Goes[6]

Accepted: 21 February 2022
© The Author(s), under exclusive licence to Springer Science+Business Media, LLC, part of Springer Nature 2022

Abstract

Up to 40% of donor corneas are deemed unsuitable for transplantation, aggravating the shortage of graft tissue. In most cases, the corneal extracellular matrix is intact. Therefore, their decellularization followed by repopulation with autologous cells may constitute an efficient alternative to reduce the amount of discarded tissue and the risk of immune rejection after transplantation. Although induced pluripotent (hiPSCs) and orbital fat-derived stem cells (OFSCs) hold great promise for corneal epithelial (CE) reconstruction, no study to date has evaluated the capacity of decellularized corneas (DCs) to support the attachment and differentiation of these cells into CE-like cells. Here, we recellularize DCs with hiPSCs and OFSCs and evaluate their differentiation potential into CE-like cells using animal serum-free culture conditions. Cell viability and adhesion on DCs were assessed by calcein-AM staining and scanning electron microscopy. Cell differentiation was evaluated by RT-qPCR and immunofluorescence analyses. DCs successfully supported the adhesion and survival of hiPSCs and OFSCs. The OFSCs cultured under differentiation conditions could not express the CE markers, TP63, KRT3, PAX6, and KRT12, while the hiPSCs gave rise to cells expressing high levels of these markers. RT-qPCR data suggested that the DCs provided an inductive environment for CE differentiation of hiPSCs, supporting the expression of *PAX6* and *KRT12* without the need for any soluble induction factors. Our results open the avenue for future studies regarding the in vivo effects of DCs as carriers for autologous cell transplantation for ocular surface reconstruction.

Keywords Cornea · Decellularization · Human induced pluripotent stem cells · Orbital fat-derived stem cells · Differentiation · Corneal epithelial cells

Dawidson Assis Gomes and Alfredo Miranda de Goes contributed equally to this work.

✉ Thaís Maria da Mata Martins
thaismmmartins@gmail.com

[1] Department of Morphology, Institute of Biological Sciences, Federal University of Minas Gerais, Avenida Presidente Antônio Carlos, 6627, Belo Horizonte, Minas Gerais 31270-901, Brazil

[2] Department of Genomic Sciences and Biotechnology, Catholic University of Brasilia, QS 07 – Lote 01, EPCT - Taguatinga, Brasília, Distrito Federal 71966-700, Brazil

[3] Faculty of Medicine, University of Brasilia, Campus Universitário Darcy Ribeiro, Brasília, Distrito Federal 70910-900, Brazil

[4] Department of Biochemistry and Immunology, Institute of Biological Sciences, Federal University of Minas Gerais, Avenida Presidente Antônio Carlos, 6627, Belo Horizonte, Minas Gerais 31270-901, Brazil

[5] Department of Biology, Minas Gerais State University, Avenida Olegário Maciel, 1427, Ubá, Minas Gerais 36502-002, Brazil

[6] Department of Pathology, Institute of Biological Sciences, Federal University of Minas Gerais, Avenida Presidente Antônio Carlos, 6627, Belo Horizonte, Minas Gerais 31270-901, Brazil

Published online: 05 March 2022

Introduction

The outermost layer of the cornea is the anterior epithelium, which is essential for ocular surface integrity, and corneal transparency. The anterior epithelium is continuously renewed by limbal stem cells (LSCs) located at the limbus, the transition zone between the cornea and the sclera [1]. LSCs deficiency (LSCD), one of the most severe corneal disorders, is caused by the dysfunction or loss of LSCs, leading to persistent epithelial defects, neovascularization, corneal opacification, and subsequent loss of vision and blindness [2].

To date, transplantation of cultured LSCs or oral mucosal epithelial cells (OMECs), often using amniotic membrane or fibrin as carrier, are the most commonly used techniques to treat LSCD [2, 3]. However, these techniques have several drawbacks, such as the limited self-renewal capacity of cultured cells, the risk of potential contamination with murine 3 T3 feeder layers and other xenogeneic components used for cell cultures and/or fibrin preparation. The amniotic membrane is difficulty to manipulate and has limited transparency and low strength [4, 5]. Moreover, peripheral corneal neovascularization has been reported after OMECs transplantation, while autologous LSCs transplantation is associated with the risk of iatrogenic LSCD in the donor eye and cannot be applied to patients with bilateral LSCD [6]. On the other hand, allogeneic transplantation is associated with the risks of immune-mediated rejection and adverse effects of immunosuppression. Clinical trials investigating LSCs or OMECs transplantation have demonstrated a low long-term success rate [3, 7, 8].

The limitations of currently available treatments for LSCD have led to increasing interest in developing novel strategies for corneal epithelial (CE) reconstruction, using alternative autologous cell sources and an appropriate substrate for them [9]. With this aim, different materials have been proposed, including collagen [10], silk fibroin [11], chitosan [12], and poly(ethylene glycol) diacrylate [13]. Although these approaches have shown some success, all these materials fail to recapitulate the complex microarchitecture, biochemical composition, biomechanical and/or optical properties of the native corneal extracellular matrix (ECM) [14]. The ECM provides biological, structural, and mechanical signals that direct CE cell fate and tissue regeneration [15]. The development of human corneal decellularization techniques allow the fabrication of scaffolds with native ECM, low immunogenicity, and proper biomechanical properties [15–18]. The decellularized matrices provide a tissue-specific microenvironment for cell adhesion, proliferation, migration, and differentiation [15, 19].

Up to 40% of human donor corneas are deemed unsuitable for transplantation, mainly due to low endothelial cell density [20, 21]. The ECM from these discarded tissues could be used to produce new corneas by the decellularization/recellularization process. Thereby, the donated corneas could be used more efficiently, increasing the donor pool [22]. Nevertheless, few studies have investigated the decellularization of human corneas at this point [23].

Most corneal decellularization/recellularization studies have used animal-derived matrices, cells and/or serum, therefore limiting the clinical translation potential of such approaches, due to the risk of prion/zoonotic transmissions and xenogeneic immune response [23–28]. In the present study we repopulated decellularized human corneas (DCs) with human stem cells which were induced to differentiate into CE cells (CECs) using a xenogeneic antigen-free differentiation medium containing human serum (HS) instead of commonly used fetal bovine serum.

Recently, we reported that sodium chloride (NaCl) plus nucleases treatment of human corneas resulted in efficient decellularization and preservation of the ECM and epithelial basement membrane (EBM) ultrastructure and composition. The decellularization efficiency and the characterization of the DCs were reported in our previously published work [29]. We also showed that the EBM of DCs is a proper substrate to facilitate the differentiation process of human embryonic stem cells (hESCs) into CECs [29]. Although hESCs hold great promise for CE reconstruction in LSCD cases, challenges remain for their clinical application. Due to the unresolved ethical and immunological issues surrounding the derivation and use of hESCs, great interest has turned to the use of human induced pluripotent stem cells (hiPSCs) and mesenchymal stem cells/medicinal signaling cells (MSCs), which provide opportunities for engineering tissues with patient-specific cells, thus avoiding the risk of rejection and the complications associated with immunosuppression [30, 31]. hiPSCs represent attractive cell sources for CE engineering due to their unlimited proliferative potential and ability to differentiate into CECs [32]. Nevertheless, no study to date has evaluated the capacity of DCs to support the attachment, survival, and differentiation of hiPSCs into CECs.

Although MSCs are also of particular interest in CE tissue engineering, the results in the literature are inconclusive regarding the transdifferentiation potential of MSCs into CECs [33–36]. Human orbital fat tissues that are regularly discarded during blepharoplasty surgeries are a good source of MSCs [37]. In vivo studies have shown the CE regeneration promoted by topical administration of human orbital fat-derived stem cells (OFSCs) and the safety and immunomodulatory effects of these cells [38, 39]. In this sense, Ho et al. have shown that direct contact between OFSCs and immortalized CECs induces CE differentiation of OFSCs. However, challenges in purifying differentiated cells may limit the clinical use of this mixed-culture system [37].

Many CECs functions and processes, including adhesion, survival, migration, and differentiation are regulated by interactions between the epithelium and the underlying EBM and stroma [40]. So, we hypothesized that the human DCs might provide a suitable and instructive microenvironment for inducing OFSCs and hiPSCs differentiation into CECs. Here, for the first time, we recellularized DCs with both stem cell types and evaluated their differentiation potential into CE-like cells using animal serum-free culture conditions.

Materials and Methods

All reagents were purchased from Thermo Fisher Scientific (Waltham, MA) unless otherwise stated.

Decellularization of Human Corneas

Human donor corneoscleral buttons (n = 69) that were rejected for transplantation due to expiration date or low cell count were obtained from the MG Transplantes Eye Tissue Bank/FHEMIG, BR. The donor age ranged from 29 to 67 years old. The Research Ethics Committee of the Universidade Federal de Minas Gerais approved the study (ETIC-UFMG-n° 49967715.0.0000.5149), and it was conducted in accordance with the Declaration of Helsinki. Informed consent was obtained from the donors' relatives for the use of tissue for research purposes.

The corneas were decellularized as previously described [29]. Briefly, whole corneas were incubated in 1.5 M NaCl for 48 h (h). They were treated with Dnase/RNase 5 U/mL for 48 h, and then washed with phosphate-buffered saline (PBS) containing 1% antibiotic/antimycotic solution for 72 h. The decellularization procedure was carried out with sterile solutions, materials, and technique.

Preparation of Allogeneic Human Serum (HS)

HS was obtained from the whole blood of distinct blood-group-typed donors [41]. All donors provided informed consent according to protocols approved by the ETIC-UFMG (n° 49967715.0.0000.5149). The blood was collected with vacutainer tubes (BD Biosciences, San Jose, CA) and allowed to clot spontaneously at 4 °C. The serum was separated by centrifugation at 252 x*g* for 10 min. Different blood types from 16 healthy donors were pooled to produce the batches of HS. The HS was incubated at 56 °C for 30 min to deactivate complement and stored at −20 °C until use.

Cell Culture

The hiPSCs line DF19–9-11 T [42] (WiCell Research Institute) was cultured on Matrigel (Corning, Corning, NY) in mTeSR™1 medium (Stem Cell Technologies, Vancouver, BC). Cells were passaged using Versene solution every 4–5 days at 1:6–1:8 ratio.

Orbital fat tissues were harvested from six healthy patients ranging in age from 50 to 62 years during upper eyelid blepharoplasty at Sociedade Oftamológica de Minas Gerais, BR. The samples were collected after obtaining informed consent from the patients (ETIC-UFMG-n° 49967715.0.0000.5149). The isolation and culture of OFSCs were performed as previously described [43]. The ECM was digested with 0.1% collagenase type I in PBS at 37 °C for 1 h. After centrifugation at 252 x*g* for 10 min, the cell pellets were resuspended in basal medium and plated into cell culture flasks. The basal medium consisted of Dulbecco's modified Eagle's medium-high glucose (DMEM, Sigma-Aldrich, St Louis, MI) supplemented with 1% antibiotic/antimycotic solution, and 10% HS.

Limbal fibroblasts (LFs) were isolated from twelve human donor corneoscleral tissues (six donors aged 33–53 years old) deemed unsuitable for transplantation obtained from the MG Transplantes Eye Tissue Bank, BR (ETIC-UFMG-n° 49967715.0.0000.5149). After removing the sclera, central and peripheral cornea, the remaining limbal tissue was cut into 1-mm^2 pieces and digested with 3 mg/mL collagenase type I in PBS at 37 °C for 3 h. After centrifugation, the pellets were resuspended in the basal medium and plated into cell culture flasks [44].

OFSCs and LFs from the third passage were used for all experiments.

Characterization of OFSCs and LFs

Flow Cytometry OFSCs suspensions (5×10^5 cells) were incubated with 0.4 µg of the following mouse monoclonal (MM) antibodies: CD105-fluorescein isothiocyanate (FITC), CD73-phycoerythrin, CD90, CD45, CD14, CD19, CD34, and HLA-DR-FITC (all from BD Biosciences, San Jose, CA). After washing with PBS, the cells were incubated with Alexa Fluor 488 goat anti-mouse IgG (for unconjugated primary antibodies). Flow cytometry was performed using a Guava® EasyCyte™ 6–2 L Flow Cytometer (Merck Millipore, Darmstadt, Germany). Fifteen thousand events were acquired and analyzed using FlowJo X (Tree Star, Inc., Ashland, OR).

OFSCs Differentiation Assays OFSCs were incubated under adipogenic, osteogenic, and chondrogenic differentiation conditions for 21 days. The multilineage potential was assessed by Oil-Red O, alizarin red S, and alcian blue staining (all from Sigma-Aldrich, St Louis, MI) [45]. For adipogenic differentiation, OFSCs were cultured in basal medium supplemented with 0.5 mM isobutylmethylxanthine, 200 µM indomethacin, 1 µM dexamethasone, and 10 µM insulin

(all from Sigma-Aldrich, St Louis, MI). For osteogenic differentiation, cells were cultured in basal medium supplemented with 50 µg/mL ascorbate-2-phosphate, 10 mM β-glycerophosphate, and 0.1 µM dexamethasone (all from Sigma-Aldrich, St Louis, MI). Chondrogenic differentiation was performed in a 3D pellet culture system using the StemPro Chondrogenesis Differentiation Kit.

Immunofluorescence LFs were characterized by immunofluorescence using previously described markers [44]. After fixation with 4% paraformaldehyde, LFs were permeabilized with 0.2% Triton X-100, blocked with 1% bovine serum albumin, and incubated with the following antibodies: rabbit monoclonal anti-CD44 (1:250), MM anti-CD106 (1:10) (both from Abcam, Cambridge, MA), MM anti-p63, MM anti-cytokeratin 3/2p, goat polyclonal anti-cytokeratin 12 (1:100, all from Santa Cruz Biotechnology, Dallas, TX), rabbit monoclonal anti-collagen type I, and rabbit polyclonal anti-fibronectin (both 1:200, Rockland, Limerick, PA). The secondary antibodies used were Alexa Fluor 488 goat anti-mouse IgG, Alexa Fluor 555 donkey anti-goat IgG, and Alexa Fluor 555 goat anti-rabbit IgG (all 1:500). The nuclei were stained with 1 µg/mL Hoechst 33258 pentahydrate, and then the cells were analyzed by fluorescence microscopy (Olympus IX70, Japan).

Conditioning of CE Medium by the LFs

Confluent LFs were mitotically inactivated by incubation with 10 µg/mL mitomycin C (Sigma-Aldrich, St Louis, MI) in basal medium for 2 h at 37 °C. Afterward, the cells were incubated in basal medium for 12 h. Then, 200 µL/cm^2 CE medium was added. This medium consisted of DMEM:F12 supplemented with 10 ng/mL human epidermal growth factor, 5 µg/mL insulin, 5 µg/mL transferrin, 0.5 µg/mL hydrocortisone, 2 nmol/L tri-iodothyronine, 0.1 µg/mL cholera toxin, 0.2 nM adenine (all from Sigma-Aldrich, St Louis, MI), 1% antibiotic/antimycotic solution, and 10% HS. The limbal fibroblast-conditioned medium (LF-CM) was collected daily and replaced with fresh CE medium for 7 days. The LF-CM was pooled, centrifuged for 3 min at 180 x*g*, filtered using a 0.22 µm filter, and stored at −80 °C until use. For all experiments, LF-CM was mixed with fresh CE medium at a ratio of 3:1 [44].

In Vitro Recellularization of DCs

The DCs were incubated in DMEM:F12 medium for 24 h at 37 °C in a CO_2 incubator before cell seeding. The hiPSCs (5–6 colonies/DC) and OFSCs (1×10^4 cells/DC) were seeded on the EBM side of the DCs and cultured for 7 days in mTeSR™1 and basal medium, respectively. The number of cells used was chosen based on our previous studies regarding recellularization of DCs with hESCs and proliferation kinetics of OFSCs [29, 43]. Cell adhesion on DCs was assessed by scanning electron microscopy (SEM). Briefly, recellularized corneas were fixed with 2.5% glutaraldehyde and 2% paraformaldehyde in PBS at 4 °C overnight. The samples were postfixed in 1% osmium tetroxide in PBS for 2 h, dehydrated in a graded series of ethanol, critical point-dried (Balzers CPD-020), and coated with gold. The samples were examined by SEM at 15 kV (DSM 950 Zeiss, Jena, Germany).

Calcein-AM staining was performed to assess cell viability. The recellularized matrices were incubated with 5 µM Calcein-AM in PBS for 30 min at 37 °C. After being rinsed with PBS, the recellularized matrices were placed on glass-bottom dishes, and visualized through confocal microscopy (Zeiss LSM 880, Jena, Germany).

CE Differentiation

The hiPSCs (5–6 colonies/DC) and OFSCs (1×10^4 cells/DC) were seeded on the EBM side of the DCs. Two days after the plating, the mTeSR™1 and basal medium were replaced by LF-CM, which was changed every other day for 21 days. Cell differentiation was assessed by reverse transcription-qPCR (RT-qPCR) and immunofluorescence analyses.

RT-qPCR Total RNA was extracted from differentiating hiPSCs and OFSCs at days 3, 6, 9, 14, and 21, from undifferentiated control cells (cells at day zero of differentiation), and from hiPSCs maintained on DCs or Matrigel in mTeSR™1 medium for 7 days. RNA was extracted using Trizol and treated with DNase. First-strand cDNA was synthesized using the High-Capacity cDNA Reverse Transcription Kit. The sequences of the forward (F) and reverse (R) primers used to amplify *GAPDH* [NM_002046.5], *PAX6* [NM_000280.4], *TP63* [NM_001114982.1], *KRT12* [NM_000223.3], *KRT3* [NM_057088.2], *POU5F1* [NM_002701.5], and *SOX2* [NM_003106.3] were: 5′-ACA TCGCTCAGACACCATG-3′ (GAPDH-F′), 5′-TGTAGT TGAGGTCAATGAAGGG-3′ (GAPDH-R′); 5′-TCACAA ACACCTACAGCGCT-3′ (PAX6-F′), 5′-ATAACTCCG CCCATTCACCG-3′ (PAX6-R′); 5′-ACGAAGATCCCC AGATGATG-3′ (TP63-F′), 5′-TGCTGTTGCCTGTACGTT TC-3′ (TP63-R′); 5′-GTTATGGGGGAAGTGCCTTTGG-3′ (KRT12-F′), 5′-GCCGGAACTAGAACCAAACATG-3′ (KRT12-R′); 5′-GAGAGTGTCCGAGTGCTGTC-3′ (KRT3-F′), 5′-GCCGTAACCTCCTCCATAGC-3′ (KRT3-R′); 5′-ATGTGGTCCGAGTGTGGTTC-3′ (POU5F1-F′), 5′- GACCCAGCAGCCTCAAAATCC-3′ (POU5F1-R′); 5′- TGGGTTCGGTGGTCAAGTCC-3′ (SOX2-F′), 5′- CTG GAGTGGGAGGAAGAGGTAAC-3′ (SOX2-R′); respectively. RT-qPCR was carried out in Applied Biosystems

7500 Real-Time PCR System using Sybr Green PCR Master Mix. Relative gene expression was determined using the REST software (http://rest.gene-quantification.info), and the mathematical model proposed by Pfaffl [46]. Undifferentiated control cells were used as calibrator, and *GAPDH* was used as a reference gene.

Immunofluorescence The hiPSCs and OFSCs maintained on DCs in LF-CM for 9 days were processed for immunofluorescence as described above. The primary antibodies used were the MM anti-p63, the MM anti-cytokeratin 3/2p, and the goat polyclonal anti-cytokeratin 12. The secondary antibodies used were the Alexa Fluor 488 goat anti-mouse IgG and the Alexa Fluor 555 donkey anti-goat IgG. The recellularized matrices were placed on glass-bottom dishes and visualized through confocal microscopy (Zeiss LSM 880, Jena, Germany).

Statistical Analysis

All experiments were repeated three times with triplicate samples. Statistical analyses were performed using the pairwise fixed reallocation randomization test. The values are presented as the mean ± standard error of the mean. Differences were considered significant at $p < 0.05$.

Results

Characterization of Orbital Fat-Derived Stem Cells (OFSCs) and Limbal Fibroblasts (LFs) Isolated and Cultured in Medium Supplemented with Human Serum (HS)

The OFSCs were successfully isolated and cultured in basal medium supplemented with HS. The adherent cells were able to self-renew, displayed fusiform morphology (Fig. 1a), multilineage differentiation potential (Fig. 1b-d), and an immunophenotype consistent with MSCs (Fig. 1e). The OFSCs differentiated into adipogenic, osteogenic, and chondrogenic lineages, as demonstrated by staining of intracellular lipid droplets, mineralized matrix, and proteoglycans by Oil-Red O (Fig. 1b), alizarin red S (Fig. 1c), and alcian blue (Fig. 1d) stainings, respectively. Flow cytometry indicated that the isolated cell population expressed CD105 (99.5% ± 0.5), CD73 (99.3% ± 0.7), and CD90 (98.5% ± 0.2), and lacked the expression of hematopoietic stem cell markers: CD34 (0.7% ± 0.2), CD45 (1% ± 0.2%), CD14 (2.6% ± 0.7), CD19 (0.9% ± 0.2), and HLA-DR (2% ± 0.2) (Fig. 1e).

The isolation and culture of LFs in basal medium supplemented with HS were successful. The adherent cells displayed a characteristic fibroblast-like morphology and were able to self-renew (Fig. 1f). Immunofluorescence confirmed the fibroblastic nature of the isolated cells (Fig. 1g-n). LFs expressed CD44 (hyaluronan receptor) (Fig. 1g), collagen type I (Fig. 1h), and fibronectin (Fig. 1i), while lacking the expression of CD106 (vascular cell adhesion molecule-1) (Fig. 1j), putative limbal stem cells (LSCs) marker TP63 (Fig. 1l), and CE cell-specific keratins KRT3 (Fig. 1m) and KRT12 (Fig. 1n). LFs were successfully used to condition CE differentiation medium.

In Vitro Recellularization of DCs

The hiPSCs and OFSCs were seeded on the denuded epithelial basement membrane (EBM) of DCs and maintained for 7 days in mTeSR™1 medium and basal medium, respectively. SEM micrographs demonstrated the ability of DCs to support hiPSCs and OFSCs adhesion and culture (Fig. 2a). Both cell types were well distributed and attached throughout the anterior surface of the DCs. Cell viability was confirmed by Calcein-AM staining (Fig. 2b).

CE Differentiation and Differentiation-Inducing Effect of DCs

The ability of OFSCs and hiPSCs to differentiate into CE-like cells when seeded on DCs and cultured in limbal fibroblast-conditioned medium (LF-CM) supplemented with HS was initially evaluated by RT-qPCR (Fig. 3 a-d). No significant change was observed in the mRNA expression levels of CE markers, *TP63*, *KRT3*, *PAX6*, and *KRT12*, in OFSCs cultured under differentiation conditions in all the time points studied compared to undifferentiated control cells.

In contrast, the gene expression levels of CE markers were significantly increased in hiPSCs cultured under CE differentiation conditions compared to undifferentiated control cells (Fig. 3 a-d). *TP63* and *KRT3* mRNA levels were upregulated at days 6, 9, 14, and 21, showing almost 62- and 20-fold increase at days 21 (*TP63*) and 9 (*KRT3*), respectively. The expression levels of *PAX6* and *KRT12* were significantly increased in hiPSCs induced to differentiate in all the time points studied, showing almost 84- and 20-fold increase at day 9 for *PAX6* and *KRT12*, respectively.

The ability of the cells to differentiate into CE-like cells was also assessed by immunofluorescence, which confirmed the expression of TP63, KRT3 and KRT12 in hiPSCs seeded on DCs and cultured in LF-CM for 9 days (Fig. 3 e-g). In contrast, TP63, KRT3 and KRT12 protein expression was not observed in OFSCs cultured under the same CE differentiation conditions (Fig. 3 h-j).

For the hiPSCs induced to differentiate on DCs, the increase in the expression of CE markers was associated with downregulation of pluripotency marker genes *POU5F1* and *SOX2* at day 21 of differentiation (Fig. 4a). Immunofluorescence demonstrated the absence of POU5F1 protein expression in

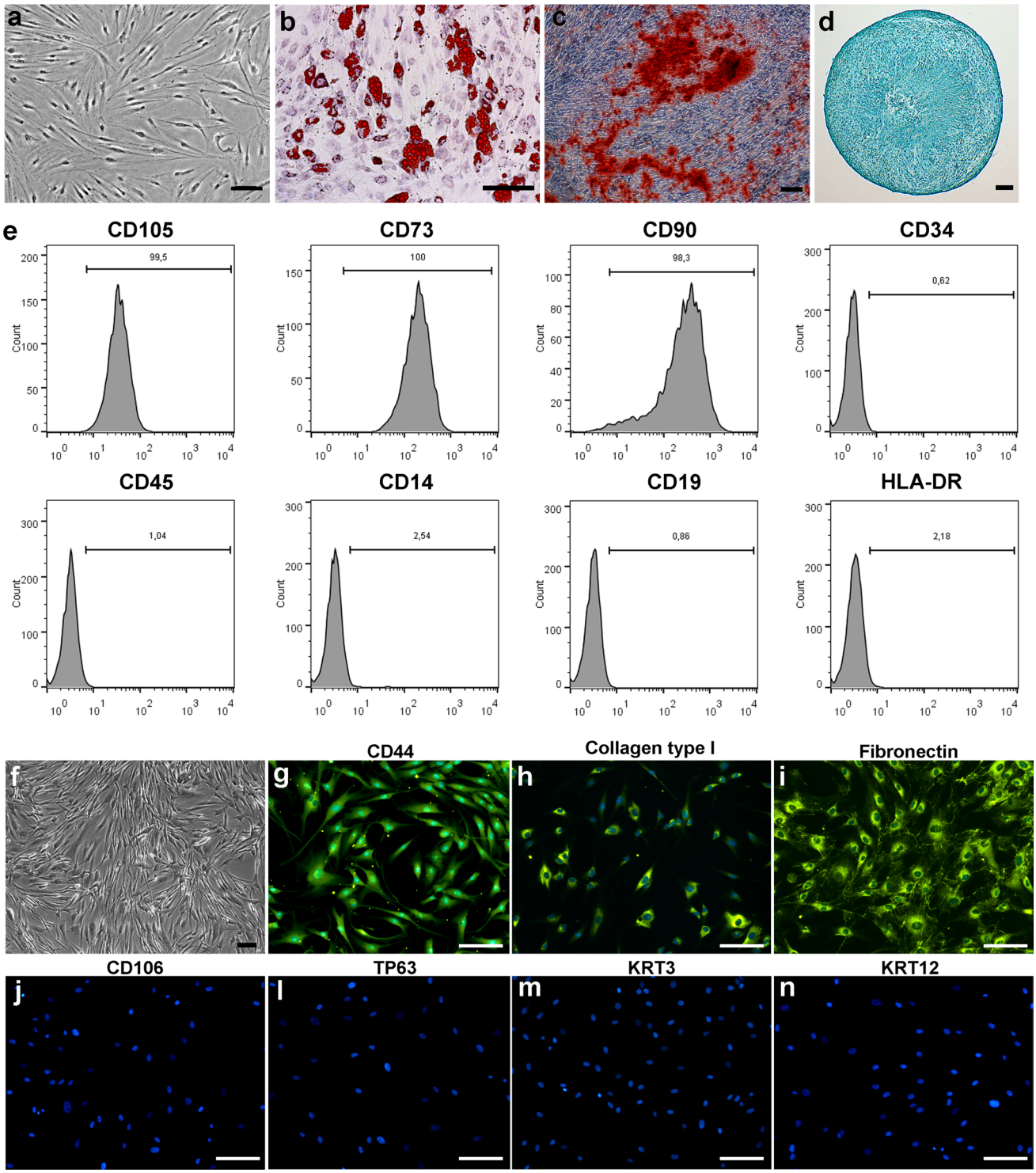

Fig. 1 Characterization of OFSCs and LFs cultured in medium supplemented with HS. (a) Fusiform morphology of OFSCs. (b) Adipogenic differentiation potential of OFSCs. Intracellular accumulation of lipid-rich vacuoles was visualized using Oil Red O staining. (c) Osteogenic differentiation capacity of OFSCs. Mineralization was visualized using alizarin red S stain. (d) Chondrogenic differentiation capacity. Alcian blue staining indicated the presence of proteoglycans in the pellet structure formed by OFSCs. (e) Cell surface antigen profiles of OFSCs by flow cytometry analysis. Expression of the mesenchymal stem cell and hematopoietic markers are depicted with representative histograms. (f) Fibroblast-like morphology of LFs. (g-n) Immunofluorescence images showing the expression of CD44 (green, g), collagen type I (green, h), fibronectin (green, i), CD106 (green, j), TP63 (green, l), KRT3 (green, m) and KRT12 (green, n) in LFs. Nuclei were stained with Hoechst (blue). Panels show representative images of three independent experiments. Scale bars: 150 µm

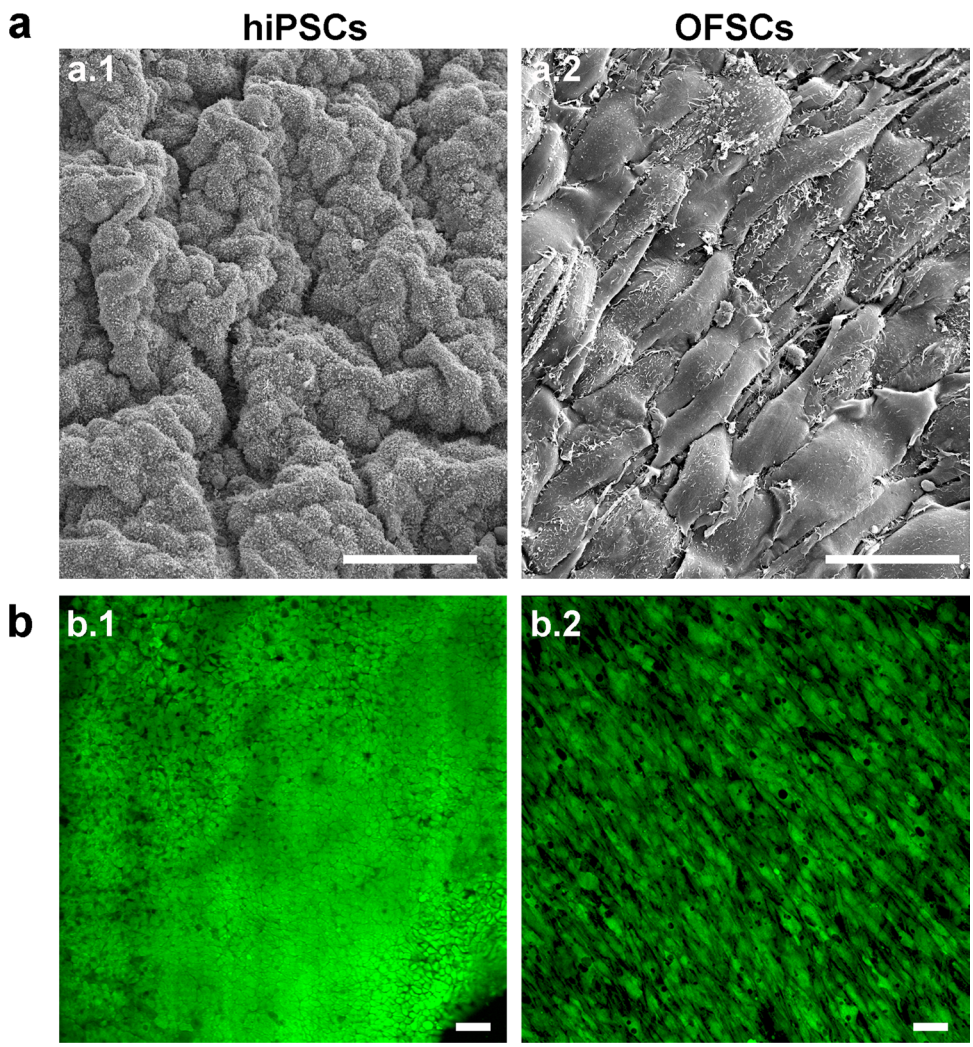

Fig. 2 In vitro recellularization of decellularized corneas. (a) Scanning electron micrographs showing the morphology of hiPSCs (a.1) and OFSCs (a.2) cultured for 7 days on decellularized corneas. (b) Confocal images showing the viability of hiPSCs (b.1) and OFSCs (b.2). Panels show representative images of three independent experiments. Scale bars: 50 µm

the hiPSCs maintained under CE differentiation conditions (Fig. 4b).

To gain additional insight on the effects of DCs alone on hiPSCs differentiation, we evaluated the gene expression of pluripotency and CE markers in the absence of any soluble differentiation factors. RT-qPCR was performed to compare the expression of these markers in hiPSCs cultured on DCs in mTeSR™1 medium for 7 days and cells maintained on Matrigel in the same undifferentiated culture conditions (Fig. 4c). There was no difference in the expression of *POU5F1*, *SOX2*, *TP63,* and *KRT3* between hiPSCs cultured on DCs and cells maintained on Matrigel. On the contrary, an increase in the expression of *PAX6* and *KRT12* was observed in cells cultured on DCs when compared to cells maintained on Matrigel.

Discussion

On average, 41–47% of donor corneas are deemed unsuitable for transplantation and discarded, representing significant financial waste and resulting in a longer waiting time for patients [20, 21]. The largest percentage of corneas are rejected due to poor endothelial cell density, and in most cases their ECM is structurally intact and could be used to engineer new corneas by decellularization techniques [22, 47]. Through human corneal decellularization techniques followed by repopulation with autologous cells, it is theoretically possible to transform allogenic grafts into autologous grafts, reducing the risk of immune rejection after corneal transplantation [16, 48, 49]. The

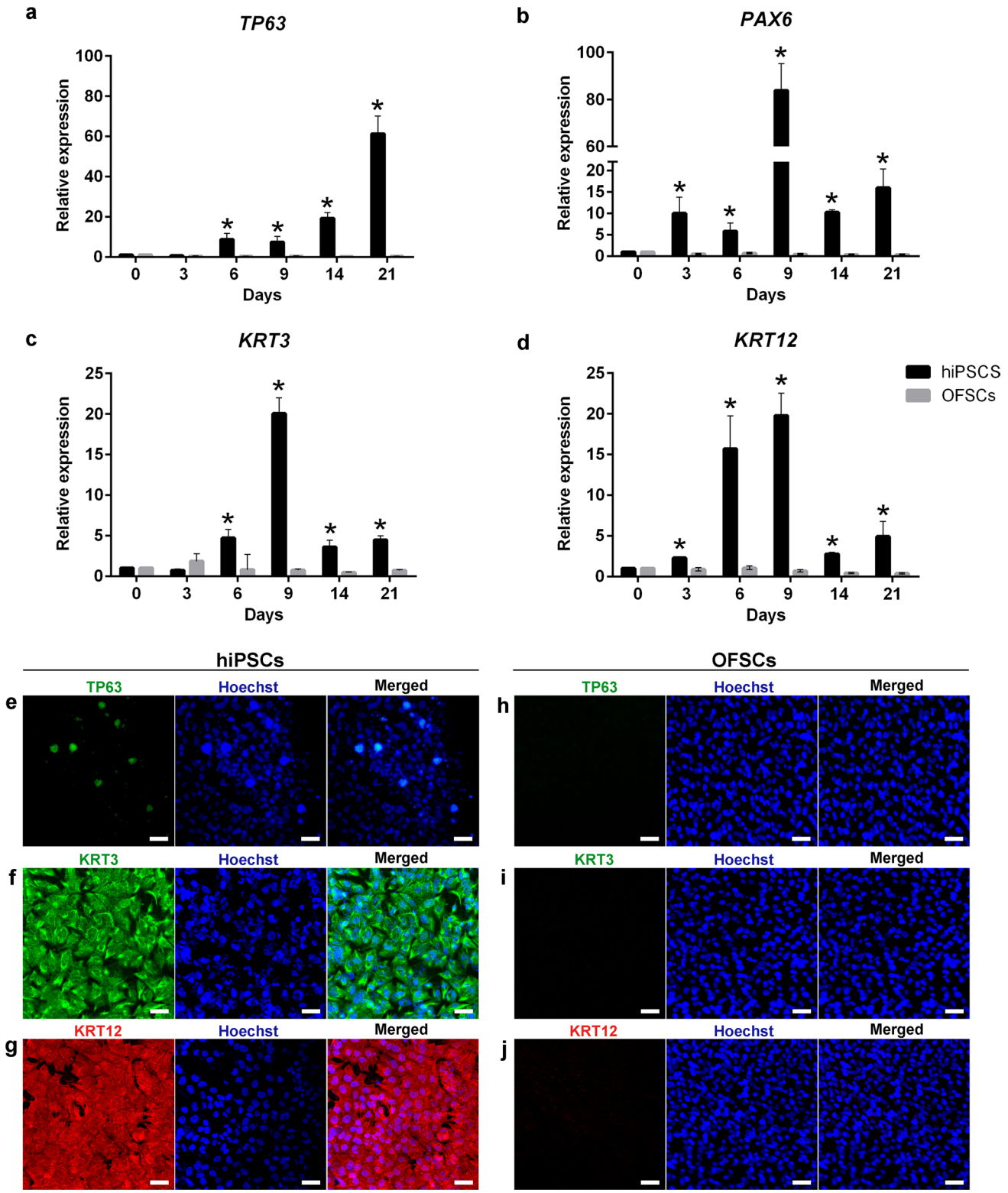

corneoscleral tissue remaining after Descemet membrane endothelial keratoplasty is another promising source of tissue for decellularization that could increase the supply of anterior lamellar grafts [16].

Albeit the availability of human corneal tissues for decellularization, most decellularization studies have been carried out using non-human animals as sources of corneas [23–28, 50, 51]. Additionally, FBS and animal-derived cells have

◂**Fig. 3** Gene and protein expression of CE markers in hiPSCs and OFSCs during the induction of differentiation. (a-d) Graphical representation of RT-qPCR analysis of *TP63* (a), *PAX6* (b), *KRT3* (c), and *KRT12* (d) expression in hiPSCs (black bars) and OFSCs (gray bars). The relative gene expression ratios between differentiated and undifferentiated cells normalized to the reference gene (*GAPDH*) were calculated using REST. Statistical significance was determined using the pair-wise fixed reallocation randomization test. Data are presented as the mean ± standard error of the mean. Experiments were performed three times independently with triplicate samples. *Compared to undifferentiated cells ($p < 0.05$). (e-j) Confocal images showing the expression of TP63 (green, e and h), KRT3 (green, f and i), and KRT12 (red, g and j) in hiPSCs (e-g) and OFSCs (h-j) after 9 days of differentiation. Nuclei were stained with Hoechst (blue). Panels show representative images of three independent experiments. Scale bars: 50 µm

been commonly used in recellularization processes [52–54]. However, xenogeneic materials face more regulatory and immunological hurdles than human counterparts, due to the risks of prion/zoonotic infections and adverse immune response [55, 56]. Xenogeneic cells express highly immunogenic epitopes to humans, and as it is unlikely that any decellularization process will remove 100% of antigenic components, residual xenoantigens may elicit an immune response [57–59]. Although porcine corneas have been the most studied tissue for decellularization so far, anatomical and biomechanical studies have indicated that they cannot be used as an appropriate model for human corneas due to important differences between them [60–63]. These are important issues to consider since recent studies have established the correlation between tissue biomechanics and corneal epithelial cell phenotype [15, 61]. Despite the advances in genome editing technologies that allow the generation of chimeric animals with humanized organs, these researches raise several ethical, religious, and safety concerns [64]. Considering all the aforementioned problems, it is clear that human materials are better choices than xenogeneic counterparts for the successful clinical application of bioengineered corneas.

In this way, our group and others have attempted to substitute FBS with pooled allogeneic HS, which can be produced in large amounts and controlled for quality according to blood bank standards [41, 43, 65–67]. We showed recently that pooled allogeneic HS enhanced MSCs proliferation without compromising their immunophenotype and differentiation capacity, thereby reducing cost and time for cell expansion under Good Manufacturing Practice conditions [41, 43]. Here, we used HS for the isolation and expansion of OFSCs and LFs, as well as for the induction of CE differentiation. OFSCs displayed morphology, differentiation potential, and immunophenotype that were in accordance with the International Society for Cellular Therapy [68]. LFs exhibited fibroblast-like morphology, expressed characteristic markers, and were successfully used to condition CE differentiation medium.

The origin of the cells used for recellularization is an important issue to consider. Non-human animal cells, immortalized cell lines, and primary human corneal cells have been used in most studies involving repopulation of DCs [17, 19, 23, 53, 69, 70]. Although primary human cells can bypass the safety concerns related to immortalized cell lines and animal-derived cells, their limited proliferation potential has hampered their clinical use. Moreover, autologous cells cannot be obtained from patients with bilateral corneal disease [2, 10]. The major advantages of using hiPSCs and OFSCs are that they are easily expandable in vitro and can be autologously sourced, rendering them non-immunogenic [34]. To our knowledge, this is the first study promoting the recellularization of DCs with OFSCs and hiPSCs. Calcein-AM staining and SEM micrographs demonstrated that DCs successfully supported the adhesion and survival of both cell types.

Deriving CECs from stem cells demands a simple, cost-effective, and preferably fast differentiation protocol. Recently, hiPSCs differentiation methods attempting to mimic whole eye development have been developed, such as self-formed ectodermal autonomous multi-zone [71, 72] and corneal organoids [73, 74], which allowed the generation of CECs and other ocular cell types. However, these methods are complex, expensive, and time-consuming since a long differentiation period (12 weeks or more) is required for the expression of CE-specific markers, and an additional cell purification step is needed. Most differentiation protocols have attempted to recreate the corneal limbal niche using murine PA6 feeder layer cells, corneal or limbal fibroblasts conditioned medium, and collagen IV-, laminin-, gelatin- or matrigel-coated surfaces [75–78]. While promising, these studies fail to consider the compositional and structural complexity of native corneal ECM and EBM, and their importance in regulating CECs function during epithelial homeostasis and regeneration [19, 40]. Previous reports on adipose tissue, heart, lung, and liver decellularization have highlighted the advantage of using natural and complex ECM niche provided by decellularized matrices as a potent factor directing tissue-specific differentiation and maturation of stem cells [79–85]. In support of these data, we recently demonstrated the efficacy of human DCs as a matrix for the induction of hESCs differentiation into CE lineage [29]. In the present study we extend this finding to hiPSCs.

TP63 is a transcription factor essential for the regenerative proliferation of LSCs, its expression is clinically relevant and serves as a hallmark of high-quality LSCs transplants [86, 87]. TP63 expression continuously increased during the differentiation process of hiPSCs peaking at day 21, suggesting a progressive increase in proliferating LSC-like cells and indicating the ability of DCs to maintain corneal epithelial stemness, which is important to renew the differentiated cells. Moreover, hiPSCs gave rise to cells

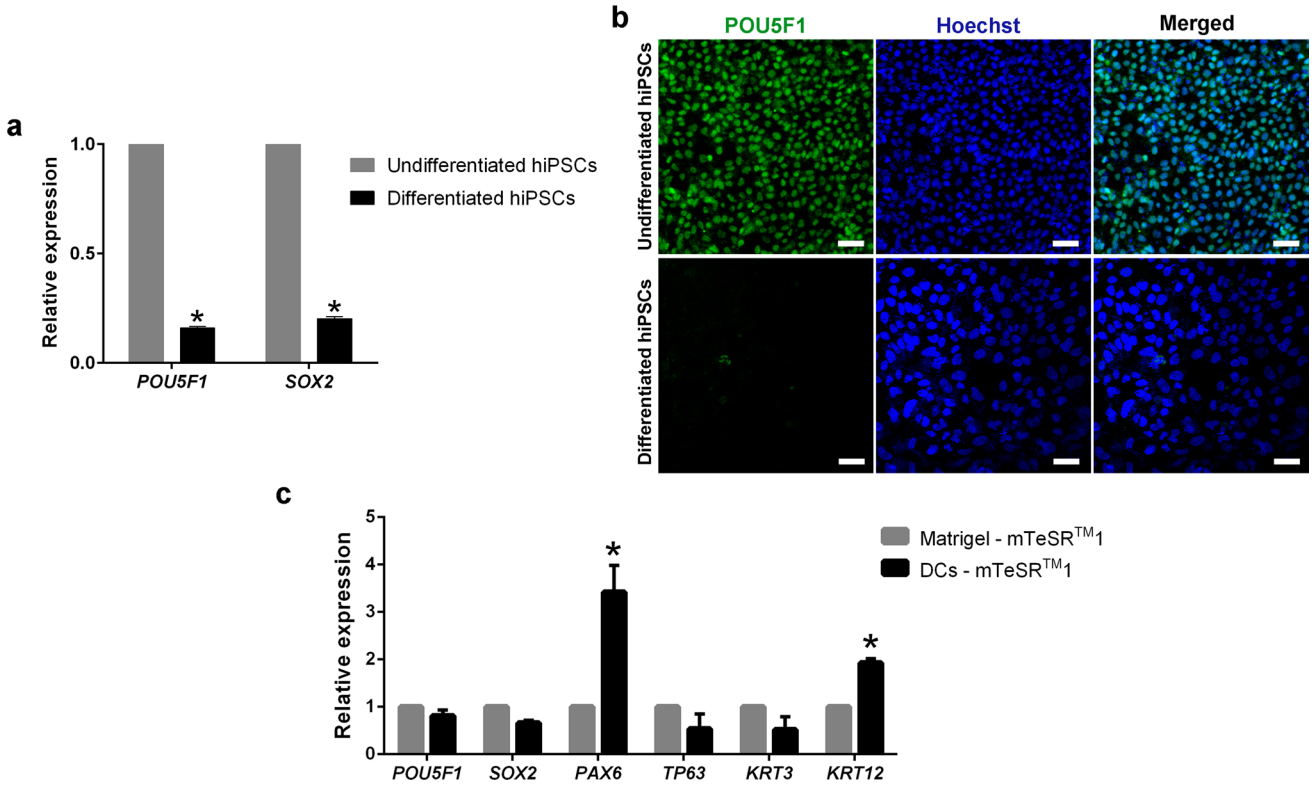

Fig. 4 Gene and protein expression of pluripotency-associated and CE markers in hiPSCs. (a) Graphical representation of RT-qPCR analysis of *POU5F1* and *SOX2* expression in undifferentiated cells and after differentiation for 21 days. The relative gene expression ratios between differentiated and undifferentiated cells were calculated using REST. *Compared to undifferentiated cells ($p < 0.05$). (b) Confocal images showing POU5F1 (green) expression in undifferentiated and differentiated cells. Nuclei were stained with Hoechst (blue). Scale bars: 50 µm. (c) Graphical representation of RT-qPCR analysis of *POU5F1*, *SOX2*, *PAX6*, *TP63*, *KRT3*, and *KRT12* expression in hiPSCs cultured on Matrigel and DCs in mTeSR™1 medium for 7 days. Relative gene expression ratios between cells cultured on DCs and Matrigel were calculated using REST. *Compared to cells cultured on Matrigel ($p < 0.05$). *GAPDH* was used as a reference gene. Statistical significance was determined using the pair-wise fixed reallocation randomization test. Data are presented as the mean ± standard error of the mean. Experiments were performed three times independently with triplicate samples

expressing high levels of mature CE markers KRT12 and KRT3 within a short time frame of 9 days, demonstrating that DCs also support CE terminal differentiation. We and others have observed that TP63 expression increased at later stages of pluripotent stem cell differentiation, while that of PAX6, KRT3, KRT12 decreased (although still upregulated compared to undifferentiated cells) [29, 75, 88], and future works to elucidate this observation will have important implications for CE tissue engineering strategies.

PAX6, the master regulator of the eye and corneal development, plays a critical role in LSCs and CE fate determination, and is a transcription factor for KRT12 gene [89]. Interestingly, our RT-qPCR data suggested that the DCs provided an inductive environment for CE differentiation of hiPSCs, supporting the expression of *PAX6* and *KRT12* without the need for any soluble induction factors.

Conversely, the OFSCs cultured under differentiation conditions could not express the CE markers. The only study reporting CE commitment of OFSCs demonstrated that direct contact with CECs is indispensable for epithelial phenotype induction of OFSCs. It showed that paracrine effects are not enough to induce the differentiation since CEC-markers were not induced by transwell non-contact co-culture system of OFSCs and CECs [37]. To date, only a few studies have shown differentiation of MSCs into CECs, and results in the literature are contradictory and inconclusive regarding this transdifferentiation potential of MSCs [31, 33, 34, 36]. Despite this, MSCs, including OFSCs, are still of particular interest in corneal tissue engineering, given their anti-inflammatory and immunomodulatory properties. They have been shown to promote regeneration, reduce inflammation and neovascularization in animal models of LSCD and corneal injury [33, 90, 91].

Thus, the demonstrations that DCs supported the adhesion and survival of OFSCs and hiPSCs as well as CE differentiation of hiPSCs in animal serum-free culture conditions open the avenue for future studies regarding the in vivo

effects of DCs as carriers for autologous cell transplantation for ocular surface reconstruction.

Acknowledgments The authors thank MG Transplantes Eye Tissue Bank/FHEMIG and Sociedade Oftamológica-MG. The microscopic data was obtained using the microscopes of "Centro de Aquisição e Processamento de Imagens" (CAPI-ICB/UFMG) and Center of Microscopy/UFMG (http://www.microscopia.ufmg.br).

Authors' Contributions Thaís Martins: Conceptualization, Methodology, Formal analysis, Investigation, Writing-original Draft. Juliana Carvalho: Conceptualization, Resources, Writing-review & editing. Pricila Cunha: Investigation, Formal analysis. Dawidson Gomes: Resources, Writing – review & editing. Alfredo Goes: Supervision, Conceptualization, Project administration, Resources. All authors approved the final version of the manuscript.

Funding This work was supported by CAPES, CNPq (167447/2017–3/404326/2012–9/471732/2012–5, 304188/2019–0), FAPEMIG (RED-00570-16, APQ-03132-18), INCT-Regenera (Brazil).

Data Availability (data transparency) Not applicable.

Code Availability (software application or custom code) Not applicable.

Declarations

Ethics Approval The Research Ethics Committee of the Universidade Federal de Minas Gerais approved the study (ETIC-UFMG n° 49967715.0.0000.5149), and it was conducted in accordance with the Declaration of Helsinki.

Consent to Participate Informed consent was obtained from the donors' relatives to use corneal tissue for research purposes. The orbital fat tissues and blood were collected after obtaining informed consent from the donors.

Consent for Publication Not applicable.

Conflict of Interest The authors indicate no potential conflicts of interest.

References

1. Cotsarelis, G., Cheng, S. Z., Dong, G., et al. (1989). Existence of slow-cycling limbal epithelial basal cells that can be preferentially stimulated to proliferate: Implications on epithelial stem cells. *Cell, 57*(2), 201–209.
2. Yazdanpanah, G., Haq, Z., Kang, K., et al. (2019). Strategies for reconstructing the limbal stem cell niche. *The Ocular Surface, 17*(2), 230–240.
3. Oliva, J., Bardag-Gorce, F., & Niihara, Y. (2020). Clinical trials of limbal stem cell deficiency treated with oral mucosal epithelial cells. *International Journal of Molecular Sciences, 21*(2), 411.
4. Rahman, I., Said, D. G., Maharajan, V. S., et al. (2009). Amniotic membrane in ophthalmology: Indications and limitations. *Eye (London, England), 23*(10), 1954–1961.
5. Nguyen, K. N., Bobba, S., Richardson, A., et al. (2018). Native and synthetic scaffolds for limbal epithelial stem cell transplantation. *Acta Biomaterialia, 65*, 21–35.
6. Kiritoshi, S., Oie, Y., Nampei, K., et al. (2019). Anterior segment optical coherence tomography angiography in patients following cultivated oral mucosal epithelial transplantation. *American Journal of Ophthalmology, 208*, 242–250.
7. Borderie, V. M., Ghoubay, D., Georgeon, C., et al. (2019). Long-term results of cultured limbal stem cell versus limbal tissue transplantation in stage III limbal deficiency. *Stem Cells Translational Medicine, 8*, 1230–1241.
8. Saghizadeh, M., Kramerov, A. A., Svendsen, C. N., et al. (2017). Concise review: Stem cells for corneal wound healing. *Stem Cells, 35*(10), 2105–2114.
9. Ghareeb, A. E., Lako, M., & Figueiredo, F. C. (2020). Recent advances in stem cell therapy for limbal stem cell deficiency: A narrative review. *Ophthalmology and therapy, 9*(4), 809–831.
10. Mikhailova, A., Ilmarinen, T., Ratnayake, A., et al. (2016). Human pluripotent stem cell-derived limbal epithelial stem cells on bioengineered matrices for corneal reconstruction. *Experimental Eye Research, 146*, 26–34.
11. Bray, L. J., George, K. A., Hutmacher, D. W., et al. (2012). A dual-layer silk fibroin scaffold for reconstructing the human corneal limbus. *Biomaterials, 33*(13), 3529–3538.
12. Liang, Y., Xu, W., Han, B., et al. (2014). Tissue-engineered membrane based on chitosan for repair of mechanically damaged corneal epithelium. *Journal of Materials Science: Materials in Medicine, 25*(9), 2163–2171.
13. Yañez-Soto, B., Liliensiek, S. J., Murphy, C. J., et al. (2013). Biochemically and topographically engineered poly(ethylene glycol) diacrylate hydrogels with biomimetic characteristics as substrates for human corneal epithelial cells. *Journal of Biomedical Materials Research Part A, 101*(4), 1184–1194.
14. Sharifi, R., Yang, Y., Adibnia, Y., et al. (2019). Finding an optimal corneal xenograft using comparative analysis of corneal matrix proteins across species. *Scientific Reports, 9*(1), 1876.
15. Palchesko, R. N., Carrasquilla, S. D., & Feinberg, A. W. (2018). Natural biomaterials for corneal tissue engineering, repair, and regeneration. *Advanced Healthcare Materials, 7*(16), e1701434.
16. El Zarif, M., Alió, J. L., Alió Del Barrio, J. L., et al. (2021). Corneal stromal regeneration: A review of human clinical studies in keratoconus treatment. *Frontiers in Medicine (Lausanne), 8*, 650724.
17. Polisetti, N., Schmid, A., Schlötzer-Schrehardt, U., et al. (2021). A decellularized human corneal scaffold for anterior corneal surface reconstruction. *Scientific Reports, 11*(1), 2992.
18. Alio, J. L., Alio Del Barrio, J. L., El Zarif, M., et al. (2019). Regenerative surgery of the corneal stroma for advanced keratoconus: 1-year outcomes. *American Journal of Ophthalmology, 203*, 53–68.
19. Shafiq, M. A., Gemeinhart, R. A., Yue, B. Y., et al. (2012). Decellularized human cornea for reconstructing the corneal epithelium and anterior stroma. *Tissue Engineering Part C: Methods, 18*(5), 340–348.
20. Rock, T., Hofmann, J., Thaler, S., et al. (2016). Factors that influence the suitability of human organ-cultured corneas. *Graefe's Archive for Clinical and Experimental Ophthalmology, 254*(1), 135–141.
21. Gavrilov, J. C., Borderie, V. M., Laroche, L., et al. (2010). Influencing factors on the suitability of organ-cultured corneas. *Eye (London, England), 24*(7), 1227–1233.
22. Wilson, S. L., Sidney, L. E., Dunphy, S. E., et al. (2016). Corneal decellularization: A method of recycling unsuitable donor tissue for clinical translation? *Current Eye Research, 41*(6), 769–782.
23. Fernandez-Perez, J., & Ahearne, M. (2019). Decellularization and recellularization of cornea: Progress towards a donor alternative. *Methods, 171*, 86–96.
24. Liu, J., Li, Z., Li, J., et al. (2019). Application of benzonase in preparation of decellularized lamellar porcine corneal stroma for

lamellar keratoplasty. *Journal of Biomedical Materials Research Part A, 107*(11), 2547–2555.
25. Isidan, A., Liu, S., Chen, A. M., et al. (2021). Comparison of porcine corneal decellularization methods and importance of preserving corneal limbus through decellularization. *PLoS One, 16*(3), e0243682.
26. Hashimoto, Y., Funamoto, S., Sasaki, S., et al. (2019). Re-epithelialization and remodeling of decellularized corneal matrix in a rabbit corneal epithelial wound model. *Materials Science & Engineering, C: Materials for Biological Applications, 102*, 238–246.
27. Sánchez-Porras, D., Caro-Magdaleno, M., González-Gallardo, C., et al. (2021). Generation of a biomimetic substitute of the corneal limbus using decellularized scaffolds. *Pharmaceutics, 13*(10), 1718.
28. Fernández-Pérez, J., Madden, P. W., Brady, R. T., et al. (2021). The effect of prior long-term recellularization with keratocytes of decellularized porcine corneas implanted in a rabbit anterior lamellar keratoplasty model. *PLoS One, 16*(6), e0245406.
29. da Mata Martins, T. M., da Silva Cunha, P., Rodrigues, M. A., et al. (2020). Epithelial basement membrane of human decellularized cornea as a suitable substrate for differentiation of embryonic stem cells into corneal epithelial-like cells. *Materials Science & Engineering, C: Materials for Biological Applications, 116*, 111215.
30. Takahashi, K., & Yamanaka, S. (2006). Induction of pluripotent stem cells from mouse embryonic and adult fibroblast cultures by defined factors. *Cell, 126*(4), 663–676.
31. Calonge, M., Pérez, I., Galindo, S., et al. (2019). A proof-of-concept clinical trial using mesenchymal stem cells for the treatment of corneal epithelial stem cell deficiency. *Translational Research, 206*, 18–40.
32. Chakrabarty, K., Shetty, R., & Ghosh, A. (2018). Corneal cell therapy: With iPSCs, it is no more a far-sight. *Stem Cell Research & Therapy, 9*(1), 287.
33. Bandeira, F., Goh, T. W., Setiawan, M., et al. (2020). Cellular therapy of corneal epithelial defect by adipose mesenchymal stem cell-derived epithelial progenitors. *Stem Cell Research & Therapy, 11*(1), 14.
34. Theerakittayakorn, K., Thi Nguyen, H., Musika, J., et al. (2020). Differentiation induction of human stem cells for corneal epithelial regeneration. *International Journal of Molecular Sciences, 21*(21), 7834.
35. Nieto-Nicolau, N., Martín-Antonio, B., Müller-Sánchez, C., et al. (2020). In vitro potential of human mesenchymal stem cells for corneal epithelial regeneration. *Regenerative Medicine, 15*(3), 1409–1426.
36. Sikora, B., Skubis-Sikora, A., Kimsa-Furdzik, M., et al. (2019). Adipose-derived stem cells undergo differentiation after co-culture with porcine limbal epithelial stem cells. *Stem Cell Research, 41*, 101609.
37. Ho, J. H., Ma, W. H., Tseng, T. C., et al. (2011). Isolation and characterization of multi-potent stem cells from human orbital fat tissues. *Tissue Engineering Part A, 17*(1–2), 255–266.
38. Lin, K. J., Loi, M. X., Lien, G. S., et al. (2013). Topical administration of orbital fat-derived stem cells promotes corneal tissue regeneration. *Stem Cell Research & Therapy, 4*(3), 72.
39. Chien, M. H., Bien, M. Y., Ku, C. C., et al. (2012). Systemic human orbital fat-derived stem/stromal cell transplantation ameliorates acute inflammation in lipopolysaccharide-induced acute lung injury. *Critical Care Medicine, 40*(4), 1245–1253.
40. Torricelli, A. A., Singh, V., Santhiago, M. R., et al. (2013). The corneal epithelial basement membrane: Structure, function, and disease. *Investigative Ophthalmology & Visual Science, 54*(9), 6390–6400.
41. Paula, A. C., Martins, T. M. M., Zonari, A., et al. (2015). Human adipose tissue-derived stem cells cultured in xeno-free culture condition enhance c-MYC expression increasing proliferation but bypassing spontaneous cell transformation. *Stem Cell Research & Therapy, 6*, 76.
42. Yu, J., Hu, K., Smuga-Otto, K., et al. (2009). Human induced pluripotent stem cells free of vector and transgene sequences. *Science, 324*(5928), 797–801.
43. Martins, T. M. M., de Paula, A. C., Gomes, D. A., et al. (2014). Alkaline phosphatase expression/activity and multilineage differentiation potential are the differences between fibroblasts and orbital fat-derived stem cells-a study in animal serum-free culture conditions. *Stem Cell Reviews and Reports, 10*(5), 697–711.
44. Ahmad, S., Stewart, R., Yung, S., et al. (2007). Differentiation of human embryonic stem cells into corneal epithelial-like cells by in vitro replication of the corneal epithelial stem cell niche. *Stem Cells, 25*(5), 1145–1155.
45. Zuk, P. A., Zhu, M., Mizuno, H., et al. (2001). Multilineage cells from human adipose tissue: Implications for cell-based therapies. *Tissue Engineering, 7*(2), 211–228.
46. Pfaffl, M. W., Horgan, G. W., & Dempfle, L. (2002). Relative expression software tool (REST) for group-wise comparison and statistical analysis of relative expression results in real-time PCR. *Nucleic Acids Research, 30*(9), e36.
47. Benetz, B. A., Stoeger, C. G., Patel, S. V., et al. (2019). Comparison of donor cornea endothelial cell density determined by eye banks and by a central reading center in the cornea preservation time study. *Cornea, 38*(4), 426–432.
48. Wilson, S. L., Sidney, L. E., Dunphy, S. E., et al. (2013). Keeping an eye on decellularized corneas: A review of methods, characterization and applications. *Journal of Functional Biomaterials, 4*(3), 114–161.
49. El Zarif, M., Alió, J. L., Alió Del Barrio, J. L., et al. (2021). Corneal stromal regeneration therapy for advanced keratoconus: Long-term outcomes at 3 years. *Cornea, 40*(6), 741–754.
50. Li, Q., Wang, H., Dai, Z., et al. (2017). Preparation and biomechanical properties of an acellular porcine corneal stroma. *Cornea, 36*(11), 1343–1351.
51. Zhou, Q., Guaiquil, V. H., Wong, M., et al. (2021). Hydrogels derived from acellular porcine corneal stroma enhance corneal wound healing. *Acta Biomaterialia, 134*, 177–189.
52. Aslan, B., Guler, S., Tevlek, A., et al. (2018). Evaluation of collagen foam, poly(l-lactic acid) nanofiber mesh, and decellularized matrices for corneal regeneration. *Journal of Biomedical Materials Research Part B: Applied Biomaterials, 106*(6), 2157–2168.
53. Lin, H. J., Wang, T. J., Li, T. W., et al. (2019). Development of decellularized cornea by organic acid treatment for corneal regeneration. *Tissue Engineering Part A, 25*(7–8), 652–662.
54. Nara, S., Chameettachal, S., Midha, S., et al. (2016). Preservation of biomacromolecular composition and ultrastructure of a decellularized cornea using a perfusion bioreactor. *RSC Advances, 6*(3), 2225–2240.
55. Kasimir, M. T., Rieder, E., Seebacher, G., et al. (2006). Decellularization does not eliminate thrombogenicity and inflammatory stimulation in tissue-engineered porcine heart valves. *The Journal of Heart Valve Disease, 15*(2), 278–286.
56. Gottipamula, S., Muttigi, M. S., Chaansa, S., et al. (2016). Large-scale expansion of pre-isolated bone marrow mesenchymal stromal cells in serum-free conditions. *Journal of Tissue Engineering and Regenerative Medicine, 10*(2), 108–119.
57. Heiskanen, A., Satomaa, T., Tiitinen, S., et al. (2007). N-glycolylneuraminic acid xenoantigen contamination of human embryonic and mesenchymal stem cells is substantially reversible. *Stem Cells, 25*(1), 197–202.
58. Dong, X., Hara, H., Wang, Y., et al. (2017). Initial study of α1,3-galactosyltransferase gene-knockout/CD46 pig full-thickness

corneal xenografts in rhesus monkeys. *Xenotransplantation, 24*(1), e12282.
59. Chen, L., Wei, L., Shao, A., et al. (2020). Immune risk assessment of residual αGal in xenogeneic decellularized cornea using GTKO mice. *Regenerative Biomaterials, 7*(4), 427–434.
60. Elsheikh, A., Alhasso, D., & Rama, P. (2008). Biomechanical properties of human and porcine corneas. *Experimental Eye Research, 86*(5), 783–790.
61. Gouveia, R. M., Lepert, G., Gupta, S., et al. (2019). Assessment of corneal substrate biomechanics and its effect on epithelial stem cell maintenance and differentiation. *Nature Communications, 10*, 1496.
62. Heichel, J., Wilhelm, F., Kunert, K. S., et al. (2016). Topographic findings of the porcine cornea. *Medical Hypothesis, Discovery and Innovation in Ophthalmology, 5*(4), 125–131.
63. Jay, L., Brocas, A., Singh, K., et al. (2008). Determination of porcine corneal layers with high spatial resolution by simultaneous second and third harmonic generation microscopy. *Optics Express, 16*(21), 16284–16293.
64. Loike, J. D., & Kadish, A. (2018). Ethical rejections of xenotransplantation? The potential and challenges of using human-pig chimeras to create organs for transplantation. *EMBO Reports, 19*(8), e46337.
65. Tonarova, P., Lochovska, K., Pytlik, R., et al. (2021). The impact of various culture conditions on human mesenchymal stromal cells metabolism. *Stem Cells International, 2021*, 6659244.
66. de Paula, A. C., Zonari, A. A., Martins, T. M. M., et al. (2013). Human serum is a suitable supplement for the osteogenic differentiation of human adipose-derived stem cells seeded on poly-3-hydroxibutyrate-co-3-hydroxyvalerate scaffolds. *Tissue Engineering Part A, 19*(1–2), 277–289.
67. Guiotto, M., Raffoul, W., Hart, A. M., et al. (2020). Human platelet lysate to substitute fetal bovine serum in hMSC expansion for translational applications: A systematic review. *Journal of Translational Medicine, 18*(1), 351.
68. Bourin, P., Bunnell, B. A., Casteilla, L., et al. (2013). Stromal cells from the adipose tissue-derived stromal vascular fraction and culture expanded adipose tissue-derived stromal/stem cells: A joint statement of the International Federation for Adipose Therapeutics and Science (IFATS) and the International Society for Cellular Therapy (ISCT). *Cytotherapy, 15*(6), 641–648.
69. Lin, Y., Zheng, Q., Hua, S., et al. (2017). Cross-linked decellularized porcine corneal graft for treating fungal keratitis. *Scientific Reports, 7*(1), 9955.
70. Islam, M. M., Sharifi, R., Mamodaly, S., et al. (2019). Effects of gamma radiation sterilization on the structural and biological properties of decellularized corneal xenografts. *Acta Biomaterialia, 96*, 330–344.
71. Shibata, S., Hayashi, R., Kudo, Y., et al. (2020). Cell-type-specific adhesiveness and proliferation propensity on laminin isoforms enable purification of iPSC-derived corneal epithelium. *Stem Cell Reports, 14*(4), 663–676.
72. Hayashi, R., Ishikawa, Y., Katori, R., et al. (2017). Coordinated generation of multiple ocular-like cell lineages and fabrication of functional corneal epithelial cell sheets from human iPS cells. *Nature Protocols, 12*(4), 683–696.
73. Foster, J. W., Wahlin, K., Adams, S. M., et al. (2017). Cornea organoids from human induced pluripotent stem cells. *Scientific Reports, 7*, 41286.
74. Susaimanickam, P. J., Maddileti, S., Pulimamidi, V. K., et al. (2017). Generating minicorneal organoids from human induced pluripotent stem cells. *Development, 144*(13), 2338–2351.
75. Cieslar-Pobuda, A., Rafat, M., Knoflach, V., et al. (2016). Human induced pluripotent stem cell differentiation and direct transdifferentiation into corneal epithelial-like cells. *Oncotarget, 7*(27), 42314–42329.
76. Shibata, S., Hayashi, R., Okubo, T., et al. (2018). Selective laminin-directed differentiation of human induced pluripotent stem cells into distinct ocular lineages. *Cell Reports, 25*(6), 1668–1679.e5.
77. Kamarudin, T. A., Bojic, S., Collin, J., et al. (2018). Differences in the activity of endogenous bone morphogenetic protein signaling impact on the ability of induced pluripotent stem cells to differentiate to corneal epithelial-like cells. *Stem Cells, 36*(3), 337–348.
78. Vattulainen, M., Ilmarinen, T., Koivusalo, L., et al. (2019). Modulation of Wnt/BMP pathways during corneal differentiation of hPSC maintains ABCG2-positive LSC population that demonstrates increased regenerative potential. *Stem Cell Research & Therapy, 10*(1), 236.
79. Grant, R., Hallett, J., Forbes, S., et al. (2019). Blended electrospinning with human liver extracellular matrix for engineering new hepatic microenvironments. *Scientific Reports, 9*(1), 6293.
80. Zhang, Y., He, Y., Bharadwaj, S., et al. (2009). Tissue-specific extracellular matrix coatings for the promotion of cell proliferation and maintenance of cell phenotype. *Biomaterials, 30*(23–24), 4021–4028.
81. Jaramillo, M., Yeh, H., Yarmush, M. L., et al. (2018). Decellularized human liver extracellular matrix (hDLM)-mediated hepatic differentiation of human induced pluripotent stem cells (hIPSCs). *Journal of Tissue Engineering and Regenerative Medicine, 12*(4), e1962–e1973.
82. Cortiella, J., Niles, J., Cantu, A., et al. (2010). Influence of acellular natural lung matrix on murine embryonic stem cell differentiation and tissue formation. *Tissue Engineering Part A, 16*(8), 2565–2580.
83. French, K. M., Boopathy, A. V., DeQuach, J. A., et al. (2012). A naturally derived cardiac extracellular matrix enhances cardiac progenitor cell behavior in vitro. *Acta Biomaterialia, 8*(12), 4357–4364.
84. Agmon, G., & Christman, K. L. (2016). Controlling stem cell behavior with decellularized extracellular matrix scaffolds. *Current Opinion in Solid State & Materials Science, 20*(4), 193–201.
85. Pati, F., Jang, J., Ha, D. H., et al. (2014). Printing three-dimensional tissue analogues with decellularized extracellular matrix bioink. *Nature Communications, 5*, 3935.
86. Di Iorio, E., Barbaro, V., Ruzza, A., et al. (2005). Isoforms of DeltaNp63 and the migration of ocular limbal cells in human corneal regeneration. *Proceedings of the National Academy of Sciences of the United States of America, 102*(27), 9523–9528.
87. Rama, P., Matuska, S., Paganoni, G., et al. (2010). Limbal stem-cell therapy and long-term corneal regeneration. *The New England Journal of Medicine, 363*(2), 147–155.
88. García, M., de la Torre, R. A., Nieto-Nicolau, N., Morales-Pastor, A., et al. (2017). Determination of the culture time point to induce corneal epithelial differentiation in induced pluripotent stem cells. *Transplantation Proceedings, 49*(10), 2292–2295.
89. Ouyang, H., Xue, Y., Lin, Y., et al. (2014). WNT7A and PAX6 define corneal epithelium homeostasis and pathogenesis. *Nature, 511*(7509), 358–361.
90. Beeken, L. J., Ting, D. S. J., & Sidney, L. E. (2021). Potential of mesenchymal stem cells as topical immunomodulatory cell therapies for ocular surface inflammatory disorders. *Stem Cells Translational Medicine, 10*(1), 39–49.
91. Galindo, S., Herreras, J. M., López-Paniagua, M., et al. (2017). Therapeutic effect of human adipose tissue-derived mesenchymal stem cells in experimental corneal failure due to limbal stem cell niche damage. *Stem Cells, 35*(10), 2160–2174.

Publisher's Note Springer Nature remains neutral with regard to jurisdictional claims in published maps and institutional affiliations.